World Academy of Science, Engineering and Technology
International Journal of Mechanical and Mechatronics Engineering
Vol:9, No:9, 2015

Line Heating Forming: Methodology and Application Using Kriging and Fifth Order Spline Formulations

Henri Champliaud, Zhengkun Feng, Ngan Van Lê, Javad Gholipour

***Abstract*—**In this article, a method is presented to effectively estimate the deformed shape of a thick plate due to line heating. The method uses a fifth order spline interpolation, with up to C^3 continuity at specific points to compute the shape of the deformed geometry. First and second order derivatives over a surface are the resulting parameters of a given heating line on a plate. These parameters are determined through experiments and/or finite element simulations. Very accurate kriging models are fitted to real or virtual surfaces to build-up a database of maps. Maps of first and second order derivatives are then applied on numerical plate models to evaluate their evolving shapes through a sequence of heating lines. Adding an optimization process to this approach would allow determining the trajectories of heating lines needed to shape complex geometries, such as Francis turbine blades.

***Keywords*—**Deformation, kriging, fifth order spline interpolation, first, second and third order derivatives, C^3 continuity, line heating, plate forming, thermal forming.

I. Introduction

METAL forming by line heating is attractive due to the process flexibility. The design and manufacture of tools in the other processes, such as stamping, pressing and bending take time and are very costly. Since line heating uses the temperature effect to deform the plates without tooling design and external forces, the small production batch becomes less costly. Francis turbine blades are made of high strength steel and are usually manufactured using a punch and die process. Since every turbine is different from one plant to another, a new tooling is required each time when a new project is launched [1]. Therefore, Francis turbine blades that have complex shapes are made in small production batch. Traditionally, the blades are shaped by hot stamping of thick plates, but due to the high tooling cost and low production rate, the manufacturing cost is dramatically high. On the other hand, shipbuilders have used efficiently a thermal gradient process to form hulls. However, the choices for selection of the heating trajectories are predominately based on the skills of the workers. As such, to transfer this approach to the manufacturing of hydroelectric assemblies, researchers have studied the effect of a specific heat trajectory on the resulting shape to automate this forming process but advanced techniques for finding the appropriate trajectories require substantial and complex calculations. Because of the huge dimension of hull, shipbuilders cannot afford these expensive press tooling. They developed an alternative contactless way of shaping plates taking advantage of the gradient of temperature created through the plate thickness by a heating source [2]. The process consists of increasing locally and quickly the temperature of one side of the plate with a heating source, such as a torch, to induce plastic strains in the plate. During cooling, the plate starts to deform such that the material in the heated region bends locally, and results in permanent deformation in the plate. An experienced and skilled worker could manage to shape a flat plate into a hull by repeating the process at specific locations over the surface of the workpiece. The research on metal forming process by line heating started by experiments in the early 1980's following by numerical modeling based on finite element method. For example, Machida et al. carried experimentally local heating on a plate [3]. McCarthy reported experimental results of the effects of main parameters on the deformation of forming by laser line heating [4]. Furthermore, Arnet and Vollertsen investigated experimentally the effects of main parameters on the bending angle of convex shape by laser forming [5]. Lately, numerical investigations have been carried out. Kyrsanidi et al. developed a three-dimensional model for laser line heating [6]. Yu et al. developed a numerical model based on finite element method for laser line heating that reduced the CPU time by zone remeshing approach [7]. As this process is complex and the deformation of single pass is usually very small, heating lines and number of pass are required to be planed before running the numerical simulations, experiments and production. In addition, the process automation becomes important to increase the productivity and reduce the operator's labor [8]. Automating the process to achieve a very accurate geometry can be overwhelming in terms of time and costs considering the countless experimental steps needed. Therefore, analytical investigations become important and are increased recently. Liu et al. developed an analytical approach to determine the scanning path for the laser heating lines design from the strain field of the curved plate [9]. Chen and Chu assessed the relationship between the stress and the temperature distributions resulting from a line heating source moving along the axial direction of a cylinder [10]. Son et al. developed an analytical model for determining the plate deformation with the heat input, material properties and plate thickness in metal forming by line heating [11]. Reutzel et al. developed a differential geometry approach based on

Henri Champliaud is with the École de Technologie Supérieure, 1100 Notre-Dame West, Montréal, QC, H3C 1K3, Canada (corresponding author; Phone: 514-396-8597; Fax: 514-396-8530; e-mail: henri.champliaud@etsmtl.ca).

Zhengkun Feng and Ngan Van Lê are with the École de Technologie Supérieure, 1100 Notre-Dame West, Montréal, QC, H3C 1K3, Canada (e-mail: zhengkun.feng@etsmtl.ca, VanNgan.Le@etsmtl.ca).

Javad Gholipour is with the National Research Council Canada, Aerospace Manufacturing, 5145 avenue Decelles, Québec, Canada, H3T 2B2, Canada (e-mail: Javad.GholipourBaradari@cnrc-nrc.gc.ca).

fundamental coefficients to predict deformation induced by multi heat line [12].

One approach, presented in this paper, is to use the known parameters of a given heating line and to apply them at different location on a numerical model. The evolution of the plate shape can then be followed without having to realize physically expensive experiments until a satisfying methodology is reached. First, for a given set of line heating parameters, a deformed shape is achieved, either by finite element simulation or experiment. A kriging model [13] is then fitted to the deformed geometry. The kriging method is used because it ensures the resulting model to pass precisely through the recorded location of actual data points or exactly through the node locations of a deformed mesh. The kriging model allows then to compute accurately the first and second derivatives for the two parametric variables of the surface all over the surface of the numerical model. Maps of first and second order derivatives are then used with a fifth order spline model with C^3 continuity constraints at each data point of the model to compute the resulting shape. Following the detailed methodology of the approach, 1D and 2D examples will be presented.

II. Methodology

A. Dual Kriging Interpolation

This method was initially developed by Krige [14] for mining exploitation in the 1950's. The kriging method was named after Matheron [15], who conducted a rigorous study of the work of Krige. A huge advantage of the kriging method in comparison with the least squares method is that it allows surfaces to pass through all the data points of a model. In addition, surface equations are continuous and derivable, i.e. the kriging method is a very interesting approach for reverse engineering problems like the one presented in this paper. The coordinates of all points on the surface are firstly recorded in a structured database (see Fig. 1), row by row, and column by column. Each point is in the form of P (s, t) where s and t denote normalized parameters. The parameterization can be discrete or a function of a distance between successive points in Euclidean coordinate system.

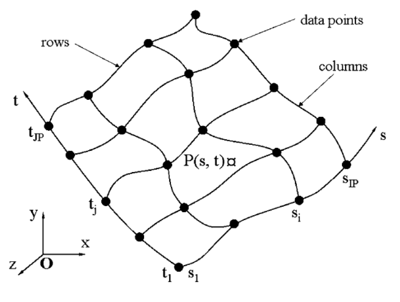

Fig. 1 Kriging interpolation of a 3D surface

Three parametric functions, x (X_i), y (X_i) and z (X_i), which describe the surface are based on dual kriging interpolation, such that they fit all the three dimensional Xi points. Each function is decomposed into the sum of two terms, in the form of a (X_i) + b (X_i), where a (X_i) represents the average behavior, called the drift, and b (X_i) is an error term called the fluctuation.

The observations u_i of a phenomenon, at data points Xi along a row, can be interpolated using the basic dual kriging model in the following form [16], [17]:

$$u(X) = \sum_1^M a_i p_i(\mathrm{X}) + \sum_1^N b_j K(|X - X_j|) \quad (1)$$

where X denotes the 3D coordinates of a point where the phenomenon is evaluated, a_i is one coefficient of the M function p_i(X) that represents the drift, and b_j is one coefficient of the N function K(|X–X_j|) that represents the fluctuation (also called the generalized covariance). |X–X_i| is the Euclidean distance between X and the data point X_i. M denotes the number of functions needed to form the drift, and N denotes the number of the data points along a row (or a column) of data points.

By using the normalized coordinates *s* and *t* to write the *x*, *y* and *z* along rows and columns, two parametric equations for each coordinate can be obtained by dual kriging. For example, for a column k:

$$X_k(s) = \sum_1^M as_i p_i(\mathrm{s}) + \sum_1^N bs_j K(|s - s_j|) \quad (2)$$

and for a row m

$$X_m(t) = \sum_1^M at_i p_i(\mathrm{t}) + \sum_1^N bt_j K(|t - t_j|) \quad (3)$$

where k (k = 1 to IP) denotes the number of columns, and m (m = 1 to JP) denotes the number of rows. The coefficients as_i, bs_j, at_i and bt_j are obtained by solving the equations x_{mk} = $x_k(s_m)$ = $x_m(t_k)$ at each data point. Finally it can be shown that:

$$x(s,t) = [x_k(\mathrm{s})]^T [x_m(\mathrm{t})] \quad (4)$$

and similar functions are used for y(s,t) and z(s,t). These functions allow the construction of a structured grid over a surface [13].

Fig. 2 presents the kriging surface of a finite element (FE) model of a plate deformed by a line heating passing across its mid length. With xyz_i the nodes of the mesh, it is well noticeable that the kriging model passes exactly by every node of the deformed plate.

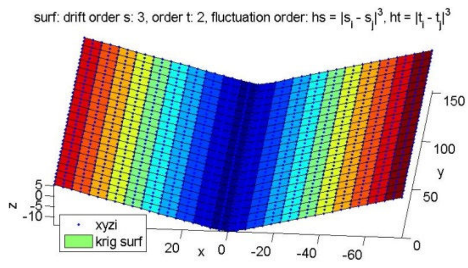

Fig. 2 Kriging of a FE model of a line heated plate

B. Fifth Order Spline Interpolation

Line heating of plates generated mainly bending distortion, and usually very small deformation occurs. Consequently, a great number of line heating are necessary to achieve a specific geometry. The idea is then to superpose a sequence of line heating over the work piece to get the intended shape. A rather simple approach for studying the step by step shape forming is to apply the same parameters extracted from the deformed plate after one single line heating pass. These parameters form a map of the first and second derivatives of the deformed shape. Applying sequentially, and at different locations, several line heating passes to an initial flat blank will progressively shape the flat plate into a 3D surface.

Bending is related to the radius curvature that can be computed from the second derivative and the first one at each point. For very small deflection, one can even assume that the radius of curvature can be approximated with the inverse of the second derivative. Then, in order to compute the new shape of a flat geometry after one or several line heating passes, the slope and the inverse of the radius of curvature must be imposed at each point. A piecewise 3rd order spline passing through a set of n point implies that the second order derivatives are equal at each interior point. Solving the system for the slopes at the interior points leads to a C^2 model which cannot describe the distorted shape since curvatures are an implied consequence of the solved system and cannot be imposed.

To ensure that slopes and curvatures can be imposed, a fifth order spline is used to link every pair of neighbor's points over the entire surface. The C^3 model can now be solved, implying that the 3rd order derivatives are equal at each point. Solving the parametric system for the new coordinates of the plate will lead to the shape of the distorted geometry. Fig. 3 shows two points P_i and P_j for which the slopes (x_i', y_i', x_j', y_j') and second derivatives (x_i'', y_i'', x_j'', y_j'') are known.

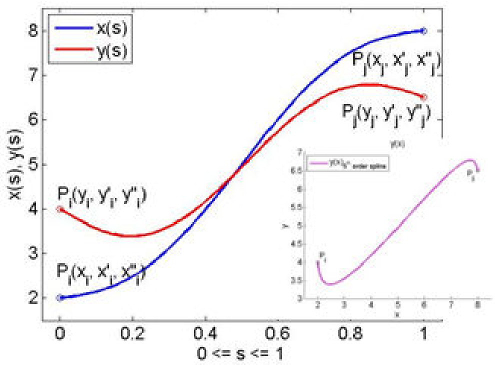

Fig. 3 Fifth order parametric spline

A fifth order parametric polynomial is represented by (5).

$$x(s) = a_0 + a_1 s + a_2 s^2 + a_3 s^3 + a_4 s^4 + a_5 s^5 \tag{5}$$

where s is a normalized parameter, i.e. $0 \le s \le 1$. The first and second derivatives with respect to s are then given by:

$$x' = a_1 + 2a_2 s + 3a_3 s^2 + 4a_4 s^3 + 5a_5 s^4 \tag{6}$$

$$x'' = 2a_2 + 6a_3 s + 12a_4 s^2 + 20a_5 s^3 \tag{7}$$

The boundary conditions at each point lead to:

$$x(s=0) = x_i \,,\; x'(s=0) = x_i' \,,\quad x''(s=0) = x_i'' \tag{8}$$

$$x(s=1) = x_i \,,\; x'(s=1) = x_i' \,,\quad x''(s=1) = x_i'' \tag{9}$$

Solving for the a_i, b_i and c_i with similar equations for y and z, will give the fifth order spline drawn from P_i to P_j as shown in Fig. 3.

A piecewise 5th order spline passing through a set of n points implies now that the third order derivatives are equal at each interior point. Solving the system for the curvatures at the interior points leads to a C^3 model. At an interior point P_i, in between neighbors points P_{i-1} and P_{i+1}, the rate of curvature is given by:

$$x_i''' = x'''(s=1) \quad \text{for the interval } P_{i-1} \text{ to } P_i \tag{10}$$

$$x_i''' = x'''(s=0) \quad \text{for the interval } P_i \text{ to } P_{i+1} \tag{11}$$

Equaling (10) to (11) lead to a system of n-2 linear equations for the unknown curvatures. Typically:

Curvature at the first point P_1:

$$3x_1'' - x_2'' = -x_1'''/3 - 12x_1' - 8x_2' - 20x_1 + 20x_2 \tag{12}$$

Curvature at an interior point P_i:

$$-x_{i-1}'' + 6x_i'' - x_{i+1}'' = 8x_{i-1}' - 8x_{i+1}' + 20x_{i-1} - 40x_i + 20x_{i+1} \tag{13}$$

Curvature at the end point P_n:

$$x_{n-1}'' - 3x_n'' = -x_n'''/3 - 8x_{n-1}' - 12x_n' - 20x_{n-1} + 20x_n \tag{14}$$

Assuming that the slopes x' and the curvatures x" at each data point are known, it is now possible to compute the coordinates of the points P_i, and then to evaluate the effect of sequence of heating lines on a geometry. If third order derivative at end points are unknown, they are simply taken as zero. Note that at least one coordinate of a data point should be given to ensure a non-singular system of equations.

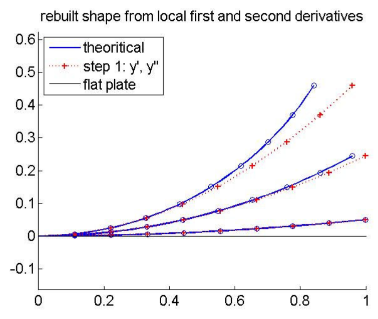

Fig. 4 y coordinates computed with a fifth order spline

III. 1D Application

A. Computing y Coordinates of a Rolled Plate

First of all a test has been made with a plate rolled according to different radius of curvature. Since the parametric equation of the rolled shaped is easy to derived, first and second order derivatives can be derived too. The first and second derivatives are then applied for different radius, step by step from an initial flat plate. Results are shown in Fig. 4.

B. Correcting x Coordinates of a Rolled Plate

It is clear that y coordinates are computed correctly but since the plate is roll bent, x coordinates do not represent correctly the deformed shape. Although the plate encounters plastic deformation, its mid plane remains elastic. Then the length of the plate should remain constant, and then the initial distance between two consecutive points should remain constant too. In order to keep constant the distance from one point to another, a parabola is used to fit three consecutive points P_i, P_j and P_k and then the arc length s of the curve along these three points is computed with (15) where a, b and c are the constants of the parabola $y(x) = ax^2 + bx + c$ passing through P_i, P_j and P_k and $\beta = dy/dx = 2ax + b$.

$$s = \int \sqrt{1+\beta^2}dx = \frac{\ln\left(\beta+\sqrt{\beta^2+1}\right)+\beta\sqrt{\beta^2+1}}{4a} \quad (15)$$

P_j and P_k are then moved along the parabola until the arc length between two consecutive points equals the initial distance separating them when the plate was flat. Fig. 5 shows the results with the corrected values for x. The new computed coordinates now match very well with the theoretical ones.

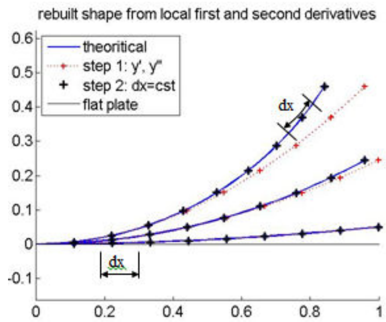

Fig. 5 Rebuilt shape with x coordinates corrected

IV. 2D Application

The algorithms presented for curves are now extended to surfaces. The system is now solved for all data points P_{ij} located at the intersection of a row i (s parameter) and a column j (t parameter). Results are presented in Figs. 6-11 for a typical pillow shape built using bicubic Bezier splines. A second example is shown in Figs. 12-17 for a blade shape surface. For these two cases, the assumption of deformation by bending without membrane stress is kept. Note that corrections have been applied to re-compute the x and y coordinates to satisfy a constant distance from point to point along an *s* or a *t* profile.

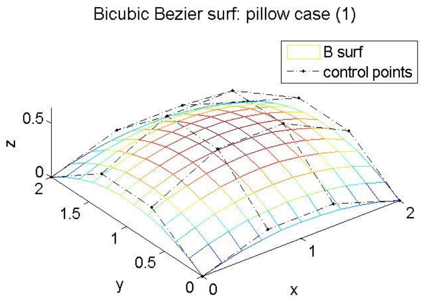

Fig. 6 Representation of a pillow surface using bicubic Bezier splines

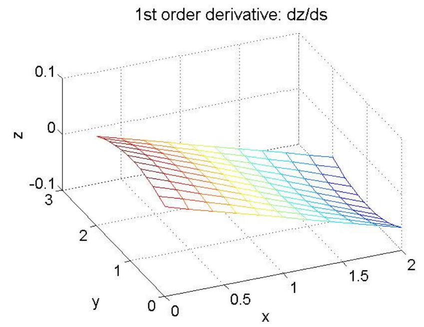

Fig. 7 Pillow shape: map of first derivatives as a function of parametric coordinate s (rows)

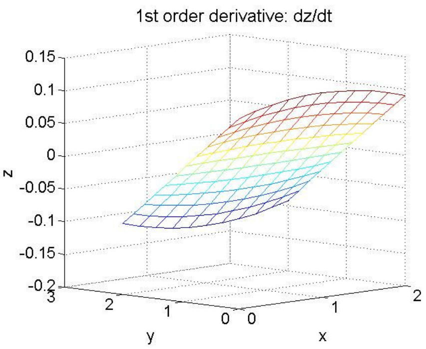

Fig. 8 Pillow shape: map of first derivatives as a function of parametric coordinate t (columns)

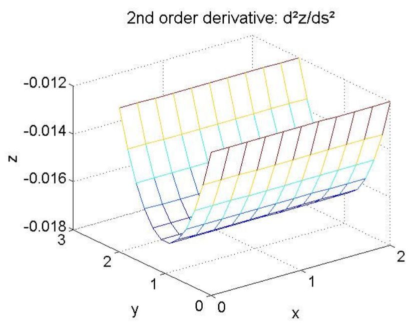

Fig. 9 Pillow shape: map of second derivatives as a function of parametric coordinate s (rows)

World Academy of Science, Engineering and Technology
International Journal of Mechanical and Mechatronics Engineering
Vol:9, No:9, 2015

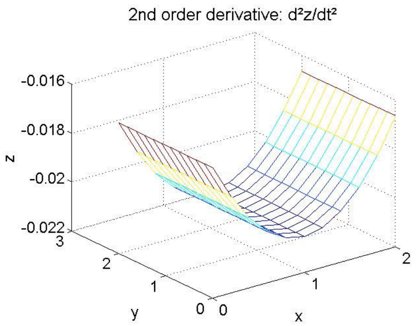

Fig. 10 Pillow shape: map of second derivatives as a function of parametric coordinate t (columns)

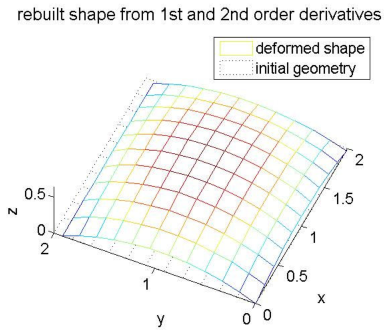

Fig. 11 Resulting pillow shape rebuilt surface using first and second order derivatives at data points

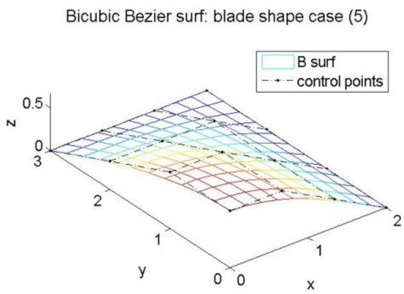

Fig. 12 Representation of a blade surface using bicubic Bezier splines

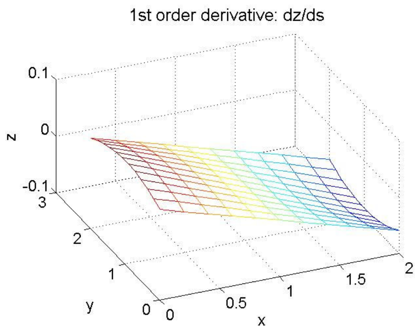

Fig. 13 Blade shape: map of first derivatives as a function of parametric coordinate s (rows)

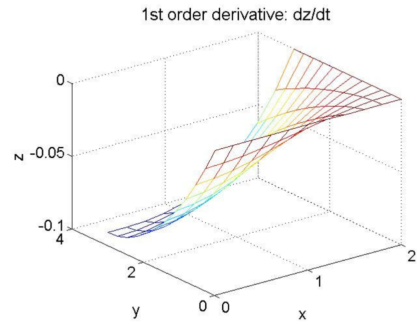

Fig. 14 Blade shape: map of first derivatives as a function of parametric coordinate t (columns) for z coordinates

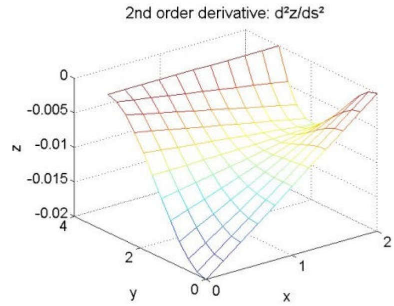

Fig. 15 Blade shape: map of second derivatives as a function of parametric coordinate s (rows) for z coordinates

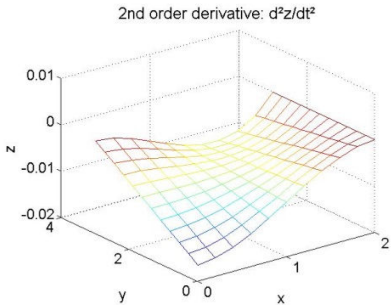

Fig. 16 Blade shape: map of second derivatives as a function of parametric coordinate t (columns) for z coordinates

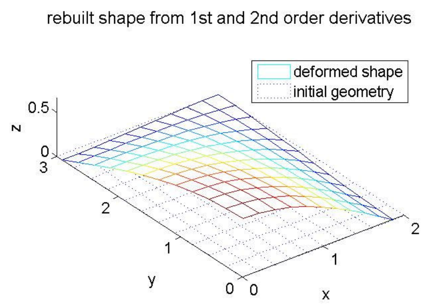

Fig. 17 Resulting blade shape rebuilt surface from first and second order derivatives at data points

Figs. 7-10 and Figs. 13-16 display the variation of first and second derivatives all over the surface for a given case, but only for z coordinates. Similar maps are computed for x and y coordinates (not shown here for brevity) and are used to re-compute the new locations of the data points and consequently the achieved deformed shape. Figs. 11 and 17 show that the rebuilt surface has been adjusted by keeping constant the initial distance in between data points of the flat plate, using a similar algorithm as presented in the previous section.

V. Conclusion

A methodology using kriging interpolation and a fifth order piecewise spline, ensuring C^3 continuity at every data points, has been developed for computing the geometry of a plate submitted to a set of heating lines. The initial parameters of the deformed geometry, which are the maps of first and second derivatives all over the surface, are applied to an initial flat plate and the resulting distorted shape is then computed. An algorithm has been also applied to keep the initial distance in between data points considering the assumption that the plate mainly encounters bending without significant membrane stresses. The algorithm can now be applied to determine how a surface could be distorted, knowing locally the effects of a given heating line on the slopes and the second derivatives. Further work, including experiments, will be developed for optimizing the set of heating line to achieve a targeted shape.

Acknowledgment

The authors thank the Natural Sciences and Engineering Research Council (NSERC), Alstom Hydro Canada Inc. and Hydro Quebec for their financial supports to this research.

References

[1] Z. Feng, H. Champliaud, M. Sabourin, and S. Morin, “Optimal blank design based on finite element method for blades of large Francis turbines,” *Simulation Modelling Practice and Theory*, vol. 36, pp. 11-21, 2013.

[2] K. Scully, “Laser line heating,” *Journal of Ship Production*, vol. 3, pp. 237-246, 1987.

[3] T. Machida, T. Okai, T. Nakagawa, and N. Taniguchi, “Forming of Thermoplastics by Utilizing their Strain Recovery Phenomena,” *CIRP Annals - Manufacturing Technology*, vol. 29, pp. 179-184, 1980.

[4] R. W. McCarthy, “Thermomechanical forming of steel plates using laser line heat,” Master Thesis, Massachusetts institute of technology, 1985.

[5] H. Arnet and F. Vollertsen, “Extending laser bending for the generation of convex shapes,” *Proceedings of the Institution of Mechanical Engineers, Part B: Journal of Engineering Manufacture*, vol. 209, pp. 433-442, 1995.

[6] A. K. Kyrsanidi, T. B. Kermanidis, and S. G. Pantelakis, “Numerical and experimental investigation of the laser forming process,” *Journal of Materials Processing Technology*, vol. 87, pp. 281-290, 1999.

[7] G. Yu, K. Masubuchi, T. Maekawa, and N. M. Patrikalakis, “FEM simulation of laser forming of metal plates,” *Journal of Manufacturing Science and Engineering, Transactions of the ASME*, vol. 123, pp. 405-410, 2001.

[8] J. S. Park, J. G. Shin, and K. H. Ko, “Geometric assessment for fabrication of large hull pieces in shipbuilding,” *CAD Computer Aided Design*, vol. 39, pp. 870-881, 2007.

[9] C. Liu, Y. L. Yao, and V. Srinivasan, “Optimal process planning for laser forming of doubly curved shapes,” *Journal of Manufacturing Science and Engineering, Transactions of the ASME*, vol. 126, pp. 1-9, 2004.

[10] L. S. Chen and H. S. Chu, “Transient thermal stresses of a composite hollow cylinder heated by a moving line source,” *Computers and Structures*, vol. 33, pp. 1205-1214, 1989.

[11] K. J. Son, J. O. Yun, Y. W. Kim, and Y. S. Yang, “Analysis of angular distortion in line-heating,” *International Journal of Mechanical Sciences*, vol. 49, pp. 1122-1129, 2007.

[12] E. W. Reutzel, L. Zhang, and P. Michaleris, “A differential geometry approach to analysis of thermal forming,” *International Journal of Mechanical Sciences*, vol. 48, pp. 1046-1062, 2006.

[13] H. Champliaud, F. Duchaine, and N. V. Lê, “Structured 3D solid mesh of complex thin parts using dual kriging interpolation,” *in 29th International conference on computers and industrial engineering*. Montreal, 2001.

[14] D. G. Krige, “Statistical approach to some basic mine valuation problems on Witwatersrand,” *Journal of the Southern African Institute of Mining and Metallurgy*, vol. 53, pp. 43-44, 1952.

[15] G. Matheron, “Intrinsic random functions and their applications,” *Advances in Applied Probability*, vol. 5, pp. 439-468, 1973.

[16] F. Trochu, “Contouring program based on dual kriging interpolation,” *Engineering with Computers*, vol. 9, pp. 160-177, 1993.

[17] C. Poirier and R. Tinawi, “Finite element stress tensor fields interpolation and manipulation using 3D dual kriging,” *Computers and Structures*, vol. 40, pp. 211-222, 1991.